LIMNOLOGY and OCEANOGRAPHY

ASLO

Limnol. Oceanogr. 9999, 2024, 1–15

doi: 10.1002/lno.12576

Effects of bottom-up factors on growth and toxin content of a harmful algae bloom dinoflagellate

Kristof Möller [1*] **Silke Thoms** [1] **Urban Tillmann** [1] **Bernd Krock** [1] **Florian Koch** [1] **Ilka Peeken** [1] **Cédric L. Meunier** [2]

[1]Alfred Wegener Institut-Helmholtz Zentrum für Polar- und Meeresforschung, Bremerhaven, Germany
[2]Alfred Wegener Institut-Helmholtz Zentrum für Polar- und Meeresforschung, Helgoland, Germany

Abstract

The toxin-producing dinoflagellate *Alexandrium pseudogonyaulax* has become increasingly abundant in northern European waters, replacing other *Alexandrium* species. *A. pseudogonyaulax* produces goniodomins and lytic substances, which can be cytotoxic toward other organisms, including fish, but we still know little about the environmental conditions influencing its growth and toxicity. Here, we investigated the impacts of different nitrogen sources and light intensities, common bottom-up drivers of bloom formation, on the growth and toxin content of three *A. pseudogonyaulax* strains isolated from the Danish Limfjord. While the growth rates were significantly influenced by nitrogen source and light intensity, the intracellular toxin contents only showed strong differences between the exponential and stationary growth phases. Moreover, the photophysiological response of *A. pseudogonyaulax* showed little variation across varying light intensities, while light-harvesting pigments were significantly more abundant under low light conditions. This study additionally highlights considerable physiological variability between strains, emphasizing the importance of conducting laboratory experiments with several algal strains. A high physiological plasticity toward changing abiotic parameters points to a long-term establishment of *A. pseudogonyaulax* in northern European waters.

The concepts of bottom-up and top-down population controls have been widely used to describe ecological mechanisms in which resource availability or grazing by predators, respectively, determine the abundance of populations (Frederiksen et al. 2006; Jacox et al. 2016). Bottom-up factors include the availability of light and macro- (e.g., C, N, P) and micronutrients (e.g., vitamins, trace metals), which are essential for microalgal growth. While intense nutrient loading of coastal zones has long been implicated as a key factor in the proliferation of algal and/or harmful algal blooms (HABs), the availability, ratio, and/or type of nutrients (e.g., inorganic vs. organic) can also influence algal community composition (Heisler et al. 2008; Anderson 2009). For instance, increases in nitrogen due to eutrophication can result in low Si : N ratios favoring non-silicious species or cause phosphorus limitation (Burson et al. 2016). Furthermore, dinoflagellates have been shown to have an advantage over other plankton groups in low nitrate and/or high dissolved organic nitrogen (DON) environments since many species are phagotrophic mixotrophs and/or are able to utilize DON but are poor competitors for nitrate (Anderson et al. 2002; Glibert 2016). Nitrate is generally suggested to favor diatom blooms, whereas other more reduced nitrogen compounds, such as ammonium or urea, are more likely to promote flagellate blooms (Bronk et al. 2007; Glibert 2016). A preference toward ammonium or urea over nitrate is driven by the energetic costs associated with the cellular metabolism of the different nitrogen sources (Cochlan and Harrison 1991; Levasseur et al. 1993). After transportation into the cell, urea is broken down enzymatically with ammonium as the final N product, and hence the reductant requirements are similar (Levasseur et al. 1993). Nitrate, on the other hand, has to be reduced to nitrite, followed by reduction to ammonium, before it can be utilized by the cell, both at the expense of energy (Thompson et al. 1989). However, in many instances, plankton grown on either ammonium or nitrate were found to have similar or

*Correspondence: kristof.moeller@awi.de

Additional Supporting Information may be found in the online version of this article.

Author Contribution Statement: K.M., U.T., B.K, F.K., and C.L.M. conceived of and designed the study. K.M. wrote the original draft while all other authors participated in reviewing and editing the manuscript. K.M, S.T., U.T., and I.P. conducted the experiments and analyzed the data.

even faster growth rates when subjected to nitrate (Leong et al. 2004; Li et al. 2011; Armstrong et al. 2018).

In addition to nutrients, light is another crucial bottom-up factor influencing the growth of microalgae, particularly for those HAB species blooming in eutrophic and often turbid environments, such as *Aureococcus anophagefferens* (Gobler et al. 2011) or *Karlodinium veneficum* (Coyne et al. 2021).

While the frequency and intensity of HABs have been increasing globally, factors responsible for bloom initiation and factors governing their toxicity are still poorly understood (Heisler et al. 2008; Anderson 2009). HABs are primarily caused by dinoflagellates, including many species of the genus *Alexandrium*, which produce various phycotoxins (Long et al. 2021). Some of these toxins can directly affect other protistan species, but others can be transferred through the food web and subsequently accumulate in higher trophic levels (e.g., in bivalves) (James et al. 2010; Long et al. 2021).

Alexandrium pseudogonyaulax, originally described from the Thau Lagoon in France (Biecheler 1952), has been increasingly prevalent in northern European waters, replacing other previously dominating *Alexandrium* species such as *Alexandrium ostenfeldii* (Kremp et al. 2019; Karlson et al. 2021). However, environmental factors that promoted this proliferation remain unresolved. This proliferation may be especially problematic as *A. pseudogonyaulax* is known to produce the phycotoxins goniodomins (GDs) (Zmerli Triki et al. 2016), which belong to a class of macrocyclic secondary polyketides including a lactone group sensitive to hydrolysis (Sharma et al. 1968; Harris et al. 2020). GDs are cytotoxic, likely due to their disturbance of the actomyosin ATPase activity and the F-actin meshwork (Terao et al. 1989; Furukawa et al. 1993; Espiña et al. 2016). *Alexandrium monilatum*, another GD producer, is also cytotoxic toward a variety of organisms, suggesting that *A. pseudogonyaulax* has a similar toxicity (Hsia et al. 2006; May et al. 2010). In addition, *A. pseudogonyaulax* also produces lytic substances that aid in mixotrophic feeding (Blossom et al. 2012, 2017), as many species of *Alexandrium* (Long et al. 2021). However, these substances have not been structurally elucidated yet and the extent to which GDs or lytic substances are responsible for the observed toxicity is unknown (Ma et al. 2011; Long et al. 2021). Several studies have investigated the effects of bottom-up factors on the toxin content of other *Alexandrium* species (Ogata et al. 1987; Béchemin et al. 1999; Parkhill 1999; Leong et al. 2004; Griffin et al. 2019), highlighting a diverse response to different bottom-up factors and underlining significant inter- and intraspecific variability of HAB species. In contrast, there is limited information available about the effects of different bottom-up factors on the physiology of *A. pseudogonyaulax* and their subsequent impact on toxin production (Zmerli Triki et al. 2015, 2016).

This study aimed to examine the impacts of light availability and different nitrogen sources on primarily the growth and toxin content of three northern European *A. pseudogonyaulax* strains isolated from the western Danish Limfjord through conducting bottle incubation experiments. In addition, it aimed to assess whether varying light intensities affect the photophysiological and pigment response of *A. pseudogonyaulax*.

Material and methods

Cell isolations

All three *A. pseudogonyaulax* strains (L2-D2 (A), L4-B1 (B), L4-B9 (C)) used in this study were established by micropipette isolation from live net tow samples under a M5A stereomicroscope (Wild) during an expedition with the R/V *Uthörn* in August 2020 in the western Danish Limfjord close to Thyborøn. The isolated single cells were transferred into 96-well tissue culture plates (TPP), each containing 250 μL of K medium (Keller et al. 2007) prepared from 0.2 μm sterile-filtered seawater from the sampling location. All strains were identified as *A. pseudogonyaulax* by cellulose staining with solophenyl flavine and observation under an inverted fluorescence microscope (Chomérat et al. 2017).

Culture maintenance

The non-axenic stock cultures were maintained under semi-batch conditions, at 20 °C, 25 PSU salinity, and 80 μmol photons m^{-2} s^{-1} (photon flux densities [PFDs]) of cool fluorescent light on a 16 : 8 h light : dark cycle. Salinity was measured on a benchtop conductivity meter (Symphony SB80PC; VWR) and converted to practical salinity units according to the standard electrical conductivity method 2520. PFDs were measured inside of the culture bottles with a light sensor (ULM-500; Walz GmbH). Stock cultures were diluted every other week to keep cells in the exponential growth phase (GP). All K/2 media (K media with half of the original nutrient concentrations, pH 8.1, 441 μmol L^{-1} NO_3^-, 25 μmol L^{-1} NH_4^+) employed in the present study was prepared from the same batch of aged seawater collected from the German North Sea near Helgoland. The original K-medium receipt was modified by replacing the organic phosphorus source with 3.62 μmol L^{-1} Na_2HPO_4. Ambient concentrations of NO_3^-, NH_4^+, and PO_4^{3-} in this seawater were 5.6, 4.6, and 0.178 μmol L^{-1}, respectively.

Experimental design

Nitrogen experiment

The impact of four different nitrogen treatments (N-deplete, NH_4^+, NO_3^-, and urea) on the growth and toxin content of two *A. pseudogonyaulax* strains (A and B) were investigated by means of bottle incubation experiments. The N-deplete treatment consisted of an aged seawater K/2 medium without any nitrogen addition. Cells were preconditioned for 2 weeks in the K/2 medium only containing the corresponding experimental nitrogen source (50 μmol L^{-1}, NH_4^+, NO_3^-, or urea), while cells in the N-deplete treatment were preconditioned in K/2 medium.

Then, exponential phase cells were collected by gently filtering over a 20 μm mesh to reduce nutrient carryover and transferred to the incubation treatment bottles. The targeted initial cell density for all treatments was 100 cells mL^{-1}. Triplicate bottles were prepared for each treatment in 500 mL sterilized screw-top polycarbonate bottles (TPP) and incubated under the same temperature and light conditions as the stock cultures. Samples for toxin and particulate organic carbon/particulate organic nitrogen (POC/PON) (Supporting Information Section S2.1) analysis were collected at the late exponential phase and in the stationary phase as identified by reaching a plateau in the sigmoidal growth curve. The urea treatment was not sampled within the exponential GP as stagnation of growth was reached unexpectedly and upon repetition, stagnation of growth appeared at even lower cell densities insufficient for the nutrient and toxin analysis. Cell densities at the start and during the experiment were determined in duplicates by microscopic counts of cells of 0.2–2 mL Lugol's iodine-fixed subsamples taken every 2nd day. The cell size was determined at both harvest points by measuring the radius of 35–90 cells and the cell volume was calculated presuming a spherical shape ($V_{cell} = 4/3 \times \pi \times r^3_{cell}$). The NH_4^+, NO_3^-, and urea treatment received an additional recovery spike of either 50 μmol L^{-1} NH_4^+ or NO_3^- once growth stagnated or declined. All treatments of strain C died during the onset of this experiment with no identifiable cause, and hence, the nitrogen experiment was only conducted with the other two strains (A and B).

Light experiment

The influence of three different PFDs (20, 100, and 200 μmol photons m^{-2} s^{-1}) on the growth and toxin content of three *A. pseudogonyaulax* strains (A, B, and C) was investigated. Cultures were grown in K/2 medium and were preconditioned to the experimental PFDs for 2 weeks. Cultures of the 20 μmol photons $m^{-2}s^{-1}$ treatment were acclimated at 60 μmol photons $m^{-2}s^{-1}$ due to slow growth. The targeted initial cell density of all treatments was 100 cells mL^{-1}. Triplicate bottles of each treatment were prepared in 250 mL sterilized screw-top polycarbonate bottles (TPP) and incubated for a period of 20–25 d under constant temperature (20 °C). Samples for toxin, POC/PON (Supporting Information Section S2.1) and pigment (Supporting Information Section S2.2) analysis were collected in the exponential phase and toxin samples a second time in the stationary phase. In addition, chlorophyll *a* (Chl *a*) fluorescence measurements were performed on a Fast Repetition Rate fluorometer (FRRf) coupled to a FastAct laboratory system (FastOcean PTX, both from Chelsea Technologies Group) detailed in the Supporting Information Section S2.3.1. Cells of the 20 μmol photons $m^{-2}s^{-1}$ treatment were only harvested in the late exponential phase. As growth declined, low light (20 μmol photons $m^{-2}s^{-1}$) treatments of strain B and C were transferred to 60 μmol photons $m^{-2}s^{-1}$. Cell densities and cell sizes were determined as described in the Nitrogen experiment.

Toxin analysis

Toxin extraction

At both cell harvests, 25 mL of each incubation bottle were harvested by centrifugation at 3220 × *g* for 10 min (Eppendorf 5810 R). Cell pellets were re-suspended in methanol (500 μL) and transferred to FastPrep tubes containing 0.9 g lysing matrix D (Thermo-Savant). Samples were homogenized by reciprocal shaking for 45 s at maximal speed (6.5 m s^{-1}) in a FastPrep instrument (Thermo-Savant) and subsequently centrifuged for 15 min at 16,100 × *g* and 10 °C (Eppendorf 5415 R). Supernatants were transferred into spin filters (Ultra-free; Millipore) and filtered by centrifugation for 30 s at 10 °C and 5000 × *g*. The resulting filtrates were transferred to high-performance liquid chromatography (HPLC) vials and stored at −20 °C until mass spectrometric analysis.

Toxin analysis

Water was deionized and purified (Millipore Milli-Q) to 18 MΩ cm^{-1} or better quality. Formic acid (90%, p.a.), acetic acid (p.a.) and ammonium formate (p.a.) were purchased from Merck. The solvents, methanol and acetonitrile, were HPLC grade (Merck). LC-MS/MS samples were analyzed by ultrahigh-performance liquid chromatography coupled with tandem quadrupole mass spectrometry (LC-MS/MS). An alkaline elution system was used with eluent A consisting of 6.7 mmol L^{-1} aqueous NH_3 and eluent B consisting of 9 : 1 (vol : vol) acetonitrile and 6.7 mmol L^{-1} aqueous NH_3. All other chromatographic and instrumental parameters were set according to Harris et al. (2023). Quantification of GDA was performed by calculating the absolute peak areas of m/z 786.5 → 733.5 with a four-point (36.67, 366.67, 825, and 1100 pg μL^{-1} GDA) external calibration curve ($R^2 = 0.99$). Finally, toxin quotas were normalized to the cellular molar carbon content (mol GDA mol^{-1} C^{-1}) or to the cell volume (pg GDA μm^{-3}).

Data analysis and statistics

All statistical analyses and plotting of data were performed using the R 4.1.2 software (R Core Team 2021). All statistical comparisons were performed by conducting a non-parametric Kruskal–Wallis test (Kassambara 2023a) followed by a Conover–Iman post hoc test after the rejection of the null hypothesis, including a p value adjustment according to Benjamini and Hochberg ($\alpha = 0.05$) (Benjamini and Hochberg 1995). Two-factor designs, involving one factor repeatedly measured over time, were analyzed by a repeated measures ANOVA with time as a dependent and the second factor as an independent variable (Kassambara 2023*a*). In case of deviations from sphericity, a Greenhouse–Geisser correction was performed to correct the degrees of freedom and hence the F-value of the ANOVA test results. In case of a significant

interaction between treatment and time, the effect of the treatment was further analyzed at each time point by a one-way ANOVA and in case of a rejection of the null hypothesis, further pairwise *t*-tests (Kassambara 2023*a*) were performed. Effect sizes, only shown between treatments and control, were calculated as Cohen's *d* and corrected according to hedges h (Kassambara 2023*a*) and interpreted as small (< 0.2), medium (0.2–0.8), and large (> 0.8). Specific growth rates (μ d^{-1}) over the exponential phase of growth were determined by fitting the cell count data with an exponential growth model featuring a heuristic linear method (Petzoldt 2022) containing five data points (only three points for strain B in the light experiment) similar to the method of Hall et al. (2014). Briefly, this approach considers a window of five-time points (points 1–5), calculates the slope, and moves then one-time point (points 2–6) further until the maximum slope is determined. All plots were generated with ggplot2 (Wickham et al. 2019) with the help of extrafont (Chang 2023), ggthemes (Arnold 2021), ggtext (Wilke and Wiernik 2022), ggprism (Dawson 2022), ggpubr (Kassambara 2023b), and patchwork (Pedersen 2024). General data transformations were performed within the tidyverse (Wickham et al. 2019). Packages were managed with pacman (Rinker and Kurkiewicz 2018) and package citations were generated with the grateful package (Rodrigues-Sanchez and Jackson 2023).

The PFDs needed for the saturating growth rate (γ_{max}) in the light experiment were calculated from the fitted growth rates using a regular asymptotic regression (Eq. 4) through a Nelder–Mead method (Soetaert and Petzoldt 2010). Then, the minimum light saturation irradiance (I_K) was calculated as the intersection of a line, with the initial slope of the regression, with the horizontal line of γ_{max}.

$$y = a - (a - b)e^{-cx}. \quad (4)$$

Results

Nitrogen experiment

Growth responses

Both strains (A and B) of *A. pseudogonyaulax* grew on all three nitrogen sources (NH_4^+, NO_3^-, urea), yielding significantly higher growth rates over the N-deplete treatment (NH_4^+, NO_3^-: $p < 0.01$; urea: $p_A < 0.1$ and $p_B < 0.05$; Fig. 1), also reflected in large effect sizes ($d = 4.1$–6.3). Furthermore, a significant interaction between nitrogen source and time indicated a time-dependency of the nitrogen source effect (strain A: $F_{16,48} = 42.41$, $p < 0.001$, strain B: $F_{16,48} = 12.33$, $p < 0.001$). Each sampling point was separately analyzed, revealing a consistent significant growth effect of the nitrogen source (strain A: $p < 0.001$, strain B: $p < 0.05$) except on the first 2 d, which can be regarded as the lag phase. Pairwise comparisons showed that after the lag phase, mean cell counts of strain A in the NH_4^+ and NO_3^- treatments were significantly

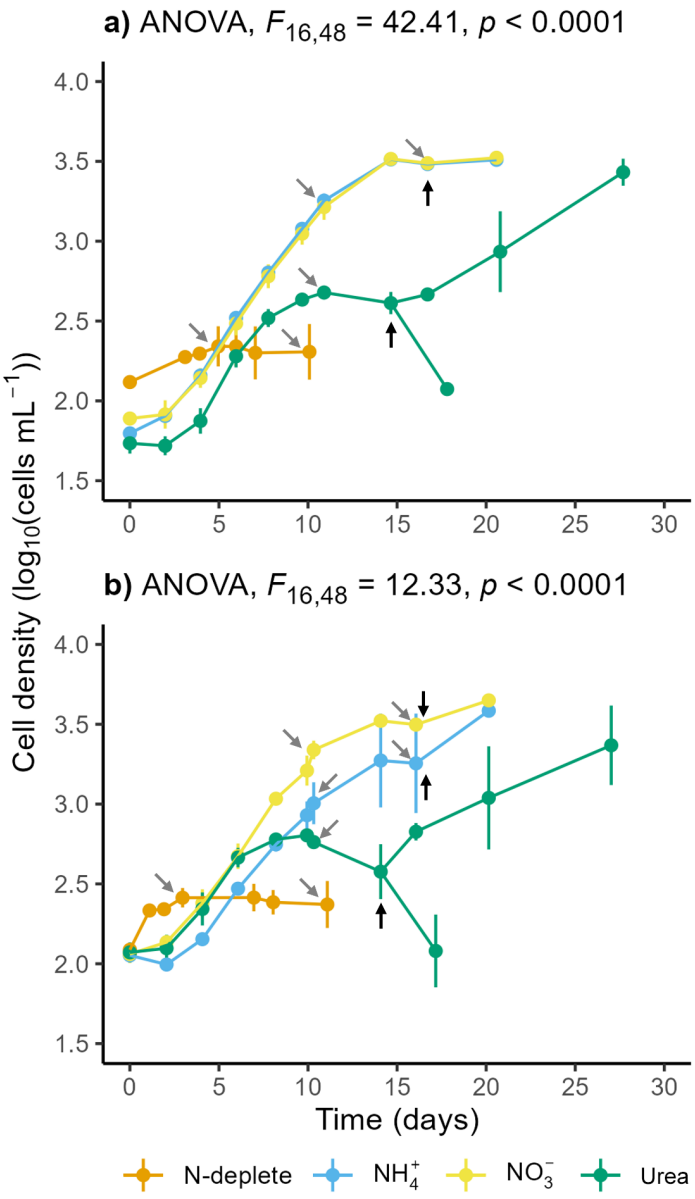

Fig. 1. Growth curves of *Alexandrium pseudogonyaulax* strains A (a: L2-D2) and B (b: L4-B1) subjected to different nitrogen sources (N-deplete, NO_3^-, NH_4^+, urea); points represent mean including standard deviations of $n = 3$ biological replicates; after a decline in cell densities (urea) or after a few days in the stationary phase (NH_4^+ and NO_3^-), aliquots from all nitrogen addition treatment flasks were spiked with additional NH_4^+ or NO_3^- at times indicated by the black arrows; particular nutrients, and toxins were sampled at times indicated by the gray arrows; test statistics correspond to a two-way repeated measures ANOVA examining the effects of time and nitrogen source on the cell counts.

($p < 0.01$) higher than in the urea treatment. Similarly, the mean cell counts of strain B in the NO_3^- treatment were significantly higher ($p < 0.01$) than the urea treatment, however only after day 8, while the mean cell counts of the NH_4^+ treatment were significantly lower than the urea treatment on days 4 and 6 ($p < 0.05$) and higher after day 10 ($p < 0.05$). No

significant differences between the NH_4^+ and the NO_3^- treatment were found at any sampling day for strain A, while for strain B the cell counts of the NO_3^- treatments were significantly higher than the NH_4^+ treatment between days 2 and 10 ($p < 0.05$).

In addition, mean growth rates of both strains in the NH_4^+ and NO_3^- treatments (Fig. 2) did not differ significantly and maximum cell densities were in the same range (NH_4^+: 3100–3800; NO_3^-: 3100–3850). In contrast, urea addition for both strains yielded significantly lower growth rates ($\leq 0.3\ d^{-1}$, $p < 0.05$) and maximum cell densities (< 1 k cells mL^{-1}, $p < 0.01$) than the inorganic nitrogen treatments. Furthermore, urea cell densities declined rapidly after reaching their maximum (Fig. 1). Growth in the urea treatment was swiftly recovered after the addition of a recovery spike of NO_3^- or NH_4^+. In contrast, further addition of nitrogen to the NH_4^+ or NO_3^- treatments resulted in no or only marginal continuative growth (Fig. 1).

Finally, the growth rates in all nitrogen treatments were the same between strains A and B ($H_1 = 0.05$–2.3, $p > 0.05$), however, the growth rate of the urea treatment was significantly higher in strain A ($H_1 = 3.86$, $p < 0.05$) compared to strain B.

Toxin quotas

Mean goniodomin A (GDA) quotas ranged between 0.74 and 6.73 pg GDA $cell^{-1}$ or 2.64×10^{-6}–3.51×10^{-5} mol GDA mol^{-1} C^{-1}. Toxin quotas of strain A (pg GDA $cell^{-1}$ and mol GDA mol^{-1} C^{-1}) were significantly higher in the stationary than in the exponential GP for all treatments ($p < 0.001$; Fig. 3). Even though the Kruskal–Wallis test for strain B yielded a p value of 0.066 (Fig. 3), subsequent post hoc tests were conducted motivated by the exploratory nature of this study. This revealed the same pattern for strain B in the NH_4^+ treatment ($p < 0.1$; Fig. 3). In the exponential GP, toxin quotas (pg GDA $cell^{-1}$ and mol GDA mol^{-1} C^{-1}) of strain A were significantly higher in the inorganic nitrogen treatments than in the N-deplete treatment (NH_4^+: $p < 0.1$, $d = 1.8$; NO_3^-: $p < 0.001$, $d = 6.1$), while they did not differ significantly for strain B. Within the stationary GP, the toxin contents (mol GDA mol C^{-1}; Supporting Information Table S3) of both strains in the inorganic nitrogen treatments were also significantly higher than in the N-deplete treatment ($p < 0.01$). However, the same pairwise comparisons did not yield significant results when analyzed as GDA per cell. In addition, within the stationary GP, toxin quotas of both strains were significantly lower in the urea (strain A: $p < 0.001$, strain B: NH_4^+: $p < 0.05$, NO_3^-: $p < 0.1$) than in the two inorganic nitrogen treatments, as well as significantly lower than in the N-deplete treatment (strain A: $p < 0.01$, $d = 2.1$; strain B: $p < 0.1$, $d = 0.3$). Finally, toxin quotas of strain B were significantly higher than those of strain A in the exponential phase of the N-deplete and the NH_4^+ treatment ($H_1 = 3.86$, $p < 0.05$).

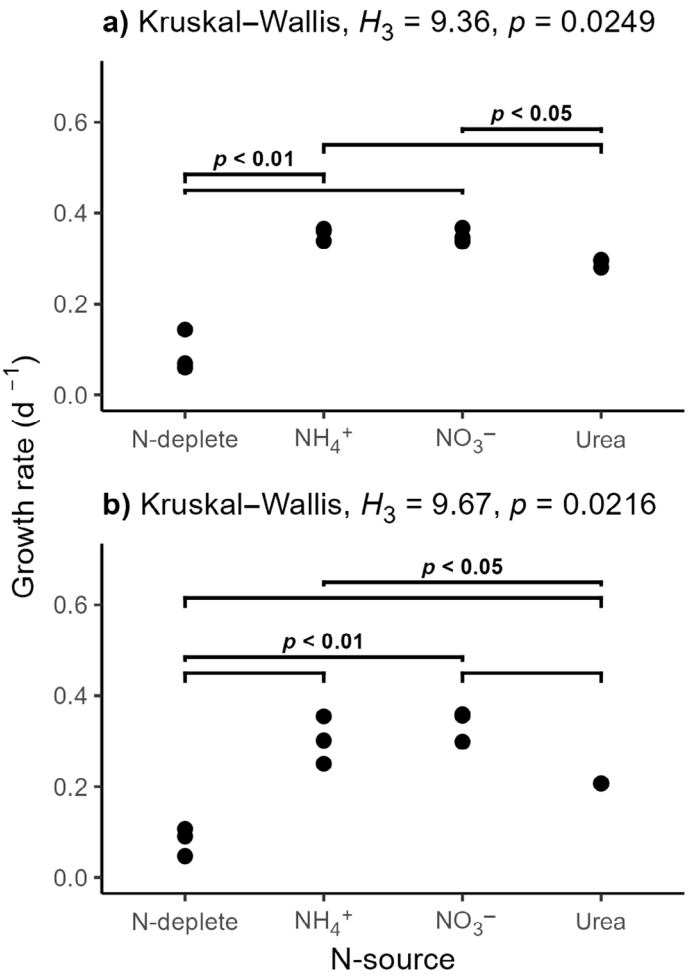

Fig. 2. Growth rates (d^{-1}) of *Alexandrium pseudogonyaulax* strains A (a: L2-D2) and B (b: L4-B1) subjected to different nitrogen sources corresponding to the growth curves of Fig. 1; points correspond to single data points of biological replicates ($n = 3$); growth rates were calculated with an exponential growth model containing five data points (2); test statistics and pairwise comparisons correspond to the Kruskal–Wallis rank sum test and to selected Conover–Iman post hoc test results, respectively.

Light experiment

Growth responses

All three strains grew under medium and high light intensities (medium light "ML": 100 μmol photons $m^{-2}s^{-1}$, high light "HL": 200 μmol photons $m^{-2}s^{-1}$), while only strain A grew continuously under low light (low light "LL": 20 μmol photons $m^{-2}s^{-1}$). A significant interaction between PFDs and time indicated a time-dependency of the light effect (strain A: $F_{18,54} = 452.21$, $p < 0.001$, strain B: $F_{14,42} = 259.64$, $p < 0.001$, strain C: $F_{18,54} = 143.15$, $p < 0.001$). Each sampling point was separately analyzed, revealing a consistent significant growth effect of the PFDs ($p < 0.001$, at day 2: $p < 0.05$), except for the initial day. Pairwise comparisons revealed that from the second day on, the mean cell counts of the ML and HL treatment were significantly higher ($p < 0.001$) than the LL treatment

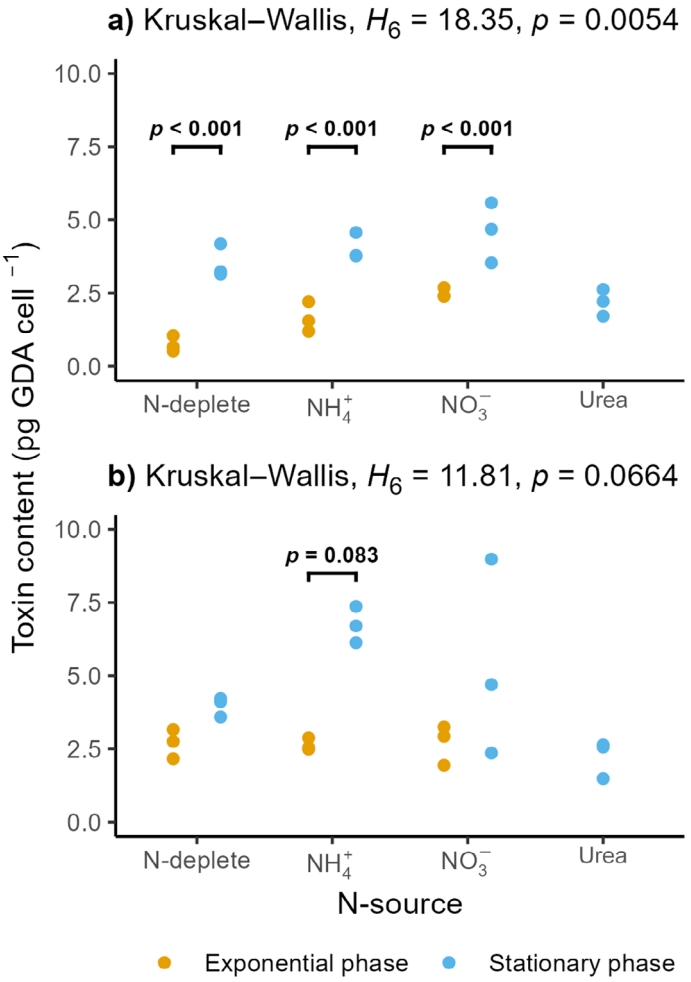

Fig. 3. Intracellular GDA toxin quotas (pg GDA cell^{-1}) of *Alexandrium pseudogonyaulax* strains A (a: L2-D2) and B (b: L4-B1) subjected to different nitrogen sources in the exponential (brown) and stationary (blue) growth phase; points correspond to single data points of biological replicates ($n = 3$); test statistics and pairwise comparisons correspond to the Kruskal–Wallis rank sum test and to selected Conover–Iman post hoc test results, respectively.

(Fig. 4). In addition, each strain grew significantly faster (strain A: $p < 0.05$, strain B/C: $p < 0.01$) in the HL than in the ML treatment, although the effect sizes were not substantially different (strain A: 59.7/40.4; strain B: 11.2/13.1; strain C: 72.0/67.5 ML/HL, respectively). Contrary, the maximum cell densities of strain A and strain B were significantly higher ($p < 0.05$) in the ML (strain A: 8800; strain B: 10,000 cells mL^{-1}) than in the HL (strain A: 6800; strain B: 9000 cells mL^{-1}) treatment, while they were the same for strain C (≈ 5600 cells mL^{-1}). In addition, all strains in ML and HL grew significantly faster (strain A/C: $p < 0.05$, strain B: $p < 0.001$ $d = 11$–72) compared to the LL treatment. The LL treatment of strain A exhibited strongly impeded growth and significantly lower cell densities at the end of the experiment (< 1.000 cells mL^{-1}, $p < 0.001$), while strains B and C did not grow continuously under LL. However, the growth of strains B and C could be stimulated by increasing the light intensity to 60 μmol photons m^{-2}s^{-1} (Fig. 4). Finally, intraspecific variabilities in the growth rates (Fig. 5) were found for the LL and ML treatment ($H_2 = 6.5$–7.2, $p < 0.05$). A subsequent post hoc analysis revealed that the growth rate of strain A was significantly higher ($p < 0.05$) than of strain B and strain C in both the LL and ML treatment, while they were the same for strain B and strain C.

A strong positive correlation (Spearmans $\rho = 0.94$, $p < 0.001$) between light intensities and growth rates was observed, which can be adequately represented by an asymptotic regression fit (Fig. 6). This analysis revealed that the minimum light saturation irradiance (I_K) was 57 μmol photons m^{-2}s^{-1} and that the maximum growth rate (γ_{max}) of *A. pseudogonyaulax* was 0.37 d^{-1}. Furthermore, the light compensation point, at which net growth is zero, was 9 μmol photons m^{-2} s^{-1}.

Toxin quotas

GDA quotas ranged between 1.0–11.8 pg GDA cell^{-1} or 7.7×10^{-6}–1.3×10^{-5} mol GDA mol C^{-1} across all treatments and strains in the light experiment (Fig. 7; Supporting Information Table S4). Toxin quotas of each strain in the stationary GP were significantly higher than in the exponential GP within the same treatment (strain A/B: $p < 0.01$, strain C: $p < 0.05$; Fig. 7). In addition, toxin quotas of strain B in the exponential GP were significantly higher in the ML and HL treatment than in the LL treatment ($p < 0.05$; Fig. 7). Significant intraspecific variabilities ($H_2 = 7.2$, $p < 0.05$) were found for all three light intensities during the exponential and stationary GP. A subsequent post hoc analysis revealed that toxin contents within each treatment of strain C were always significantly higher ($p < 0.05$) than those of strain A, which in turn were significantly higher ($p < 0.05$) compared to strain B.

Pigment composition and abundances

The following pigments were identified in *A. pseudogonyaulax* cells: Chl *a*, peridinin, β-carotene, Chl c_2, violaxanthin (only in strain A and strain B), diadinoxanthin, dinoxanthin, diatoxanthin, and zeaxanthin. While pigment ratios were similar across treatments, significant differences emerged in the molar ratios ($H_2 = 7.2$, $p < 0.05$) of light-harvesting (LH) to light-protecting (LP) pigments. The LH : LP in the LL treatment for each strain was significantly higher ($p < 0.05$) than ML and HL treatments, with approximately threefold differences (Supporting Information Table S5). More detailed results about pigment abundances can be found in the Supporting Information Section S3.2.1.

Photophysiological responses

In strain A, the ML treatment exhibited a significantly higher ($H_2 = 7.2$, $p < 0.05$) dark-adapted maximum quantum yield ($F_v F_m^{-1}$) compared to LL and HL treatment (Supporting Information Table S4). In addition, the concentration of functional PSII reaction centers (RCII) was significantly higher in

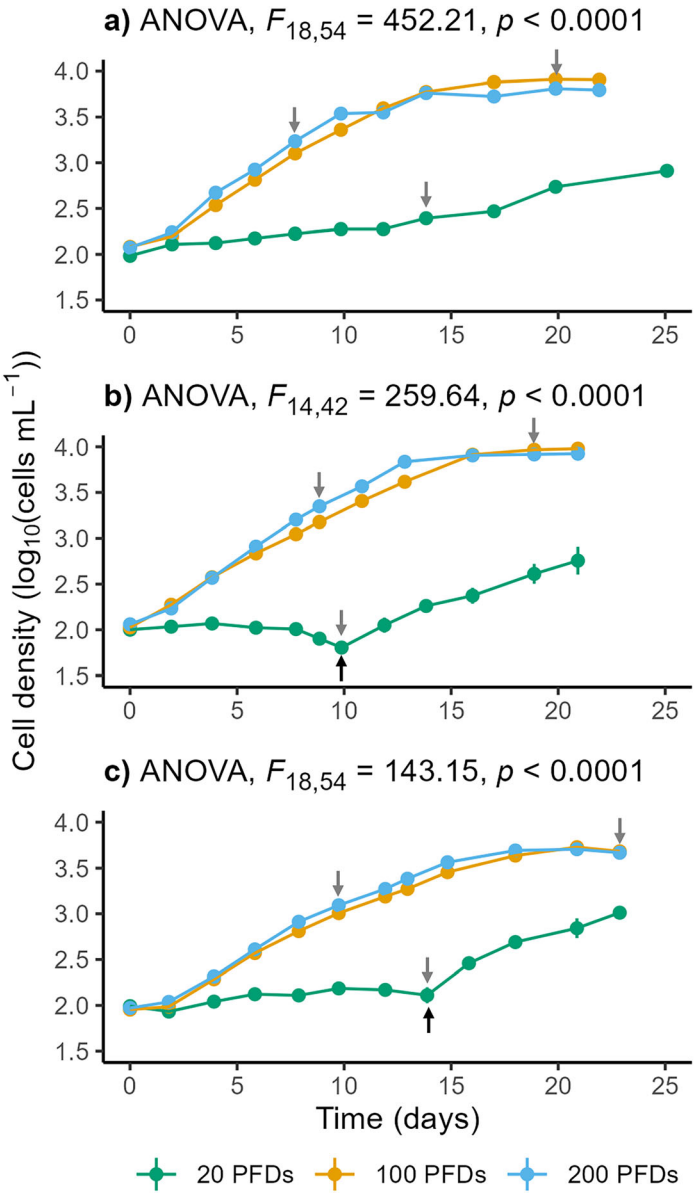

Fig. 4. Growth curves of *Alexandrium pseudogonyaulax* strains A (a: L2-D2), B (b: L4-B1), and C (c: L4-B9) subjected to different photon flux densities (20, 100, and 200 μmol photons m^{-2} s^{-1}, PFDs); points represent mean including standard deviations of $n = 3$ biological replicates; low light (20 μmol photons m^{-2}s^{-1}) treatments of strain B and C were transferred to 60 μmol photons m^{-2}s^{-1} after the onset of a decline in cell densities as indicated by the black arrow; particular nutrients, pigments and toxins were sampled at times indicated by the gray arrows; test statistics correspond to a two-way repeated measures ANOVA examining the effects of time and light intensity on the cell counts.

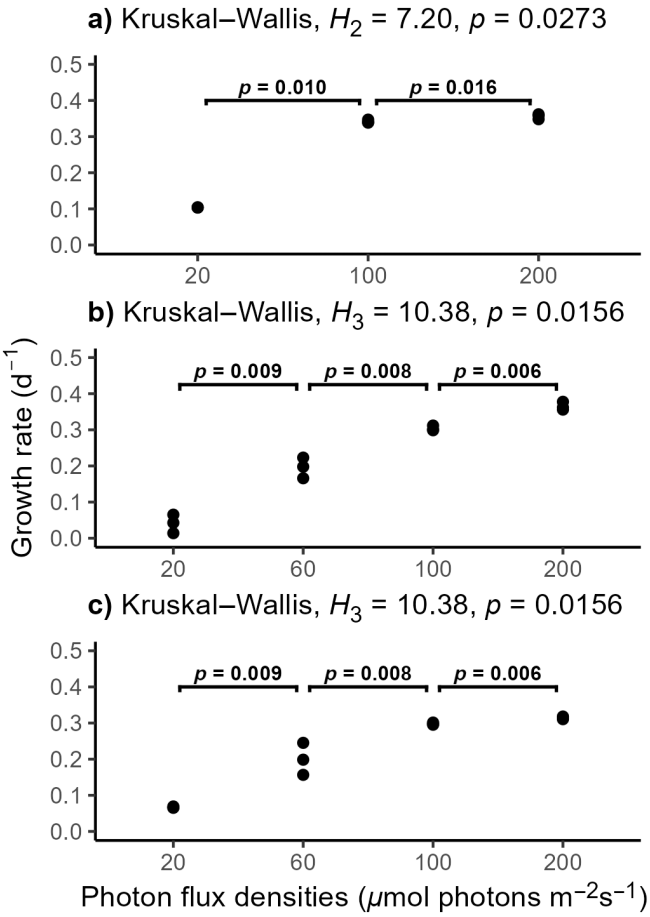

Fig. 5. Growth rates (d^{-1}) of *Alexandrium pseudogonyaulax* strains A (L2-D2), B (L4-B1), and C (L4-B9) subjected to different photon flux densities (μmol photons m^{-2} s^{-1}) corresponding to the growth curves of Fig. 4; points correspond to single data points of biological replicates ($n = 3$); growth rates were calculated with an exponential growth model containing five data points; test statistics and pairwise comparisons correspond to the Kruskal–Wallis rank sum test and to selected Conover–Iman post hoc test results, respectively.

the ML than in the HL treatment ($p < 0.001$), but RCII in the HL treatment remained significantly higher than in the LL treatment ($p < 0.05$). RCII remained the same across all treatments for strain B and C. Finally, for strain A, the maximum electron transport rate (ETR) ETR_{max} and the minimum saturating light irradiance (I_K) in the ML treatment were significantly lower ($p < 0.05$) than in the LL and HL treatment (Fig. 8; Supporting Information Table S4). In accordance, multiplying the ETR with RCII to yield the ETR_{cell} showed that ETR_{cell} increased concomitantly with the PFDs (only calculated for strain A; Fig. 8). In general, ETRs per PSII of all treatments and strains were high compared to other algal species such as green algae. Strain A was chosen to be considered in more detail within the photophysiological model due to its significant differences in RCII concentrations and ETR_{max}, consequently affecting ETR_{cell}, unlike strains B and C, which displayed similar ETR_{cell} values across all treatments (Supporting Information Fig. S1; Supporting Information Table S4). Increasing the rate constants for the mobile electron carriers plastoquinone, plastocyanin, and ferredoxin within the photophysiological model (Supporting Information Section S2.3.2) enabled to account for the potential

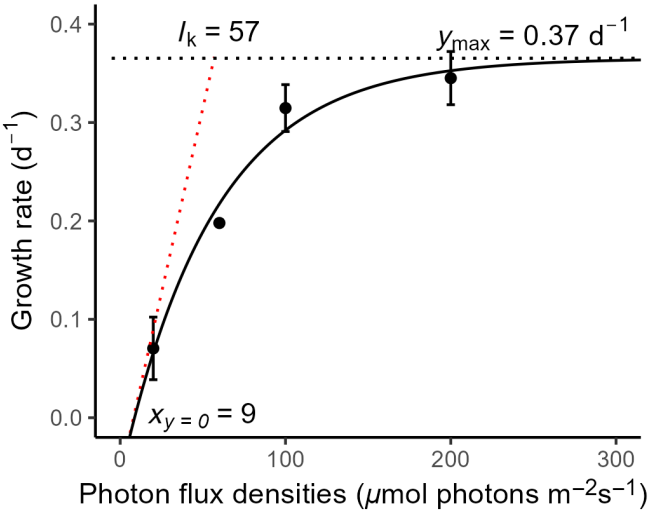

Fig. 6. Asymptotic regression analysis of the growth rates (d^{-1}) of three *Alexandrium pseudogonyaulax* strains corresponding to Fig. 5, including the minimum saturating light irradiance (I_k) and the maximum growth rate (y_{max}, d^{-1}); points correspond to the mean ($n = 3$) of the mean of each strain ($n = 3$) including standard deviations.

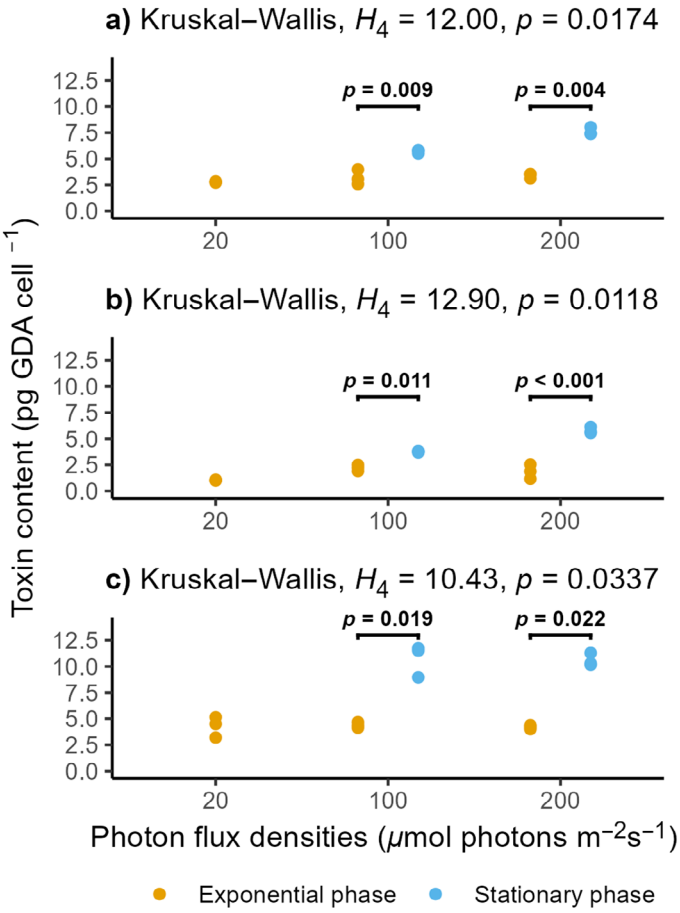

Fig. 7. Intracellular GDA toxin quotas (pg GDA cell^{-1}) of *Alexandrium pseudogonyaulax* strains A (a: L2-D2), B (b: L4-B1), and C (c: L4-B9) subjected to different photon flux densities in the exponential (brown) and stationary (blue) growth phase; points correspond to single data points of biological replicates ($n = 3$); test statistics and pairwise comparisons correspond to the Kruskal–Wallis rank sum test and to selected Conover–Iman post hoc test results, respectively.

impact of different RCII concentrations on the diffusion of the mobile electron carriers. The used parameters of this model adapted to *A. pseudogonyaulax* are shown in the Supporting Information Tables S1, S2 and more detailed information about the photophysiological response can be found in Supporting Information Section 3.2.2.

Discussion

A. pseudogonyaulax and the role of nitrogen

Nitrogen plays a crucial role in the formation of HABs and is typically the major limiting nutrient in coastal marine systems (Heisler et al. 2008; Gobler 2020), hence investigating N-preference is essential for characterizing the ecophysiology of *A. pseudogonyaulax*.

Inorganic nitrogen sources, but not urea, sustained growth

The growth response of two *A. pseudogonyaulax* strains observed in this study emphasize the complex nature of nitrogen utilization by microalgae. The nitrogen concentrations (50 μmol L^{-1}) employed in this experiment reflect maximum total nitrogen levels observed in various regions of the Limfjord such as the western Nissum Bredning, and the central Skive Fjord, Risgårde Bredning, Lovns Bredning, and Løgstør Bredning (Carstensen et al. 2013; Jakobsen and Markager 2016). While the highest growth rates (0.3–0.4 d^{-1}) were obtained when this dinoflagellate was exposed to inorganic nitrogen sources (NH_4^+ or NO_3^-), no significant differences in growth between the two nitrogen sources were detected (Figs. 1, 2). This finding suggests that *A. pseudogonyaulax* growing on nitrate may compensate for higher reductant requirements through alternative means other than a reduction in growth or that a decrease in growth was marginal and hence, undetectable (Levasseur et al. 1993). Another possibility may be that the growth rate of *A. pseudogonyaulax* is restricted by other unknown intrinsic factors and the conserved reduction potential cannot be converted to enhanced growth. Notably, while lower reduction requirements generally favor NH_4^+ over NO_3^- (Levasseur et al. 1993) no conclusions toward a nitrogen preference in the presence of both NH_4^+ and NO_3^- can be drawn.

Moreover, the growth rate of *A. pseudogonyaulax* was significantly lower when nitrogen was only available as urea (Figs. 1, 2), which is important as the Limfjord features higher organic than inorganic nitrogen concentrations (Carstensen et al. 2013). Despite initial growth, all urea treatments failed to reach high cell densities and the population started to decline before the experiment concluded. This was probably

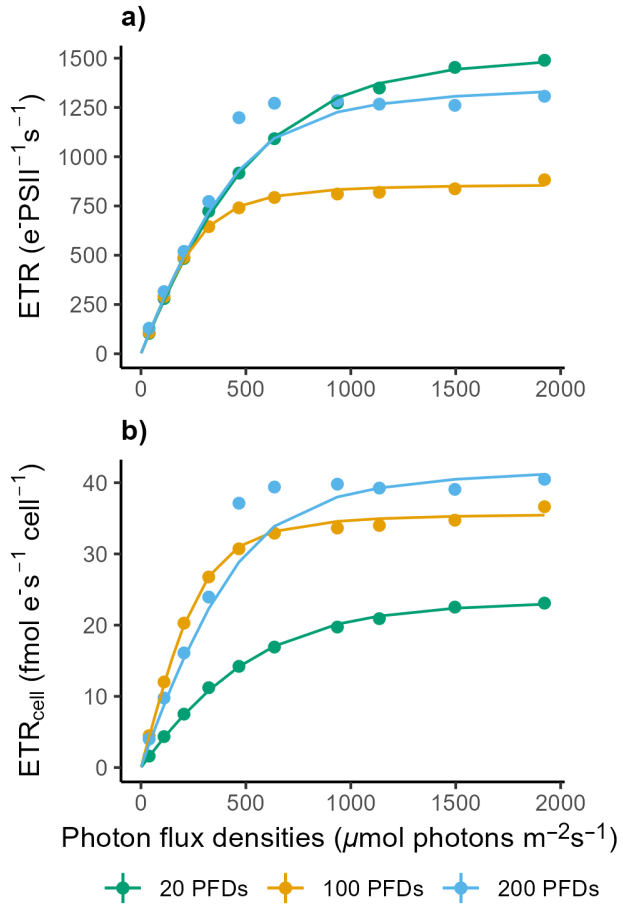

Fig. 8. Measured and calculated ETR of *Alexandrium pseudogonyaulax* strain A (L2-D2) harvested in the exponential growth phase after exposure to three different photon flux densities (PFDs), normalized to either PSII (a: ETR) or to the entire cell (b: ETR_{cell}); points refer to the measured (mean of $n = 3$) and lines to the modeled ETR, respectively.

caused by nitrogen limitation due to the inability to utilize urea as the only nitrogen source. Given that the reductant requirements of ammonium and urea are similar (Levasseur et al. 1993), it is plausible that lower growth rates in the urea treatment were caused by a reduced efficiency in cellular processes such as urea uptake and/or enzymatic conversion into NH_4^+ (Dyhrman and Anderson 2003). Dyhrman and Anderson (2003) demonstrated that *A. catenella* is able to utilize urea as the sole nitrogen source, but only in the presence of nickel hinting toward nickel-dependent urease activity. Other studies reporting the growth of *Alexandrium* species on diverse nitrogen sources, including urea, without the addition of nickel to the growth media, may therefore be attributed to varying background concentrations of nickel in the employed seawater (Leong et al. 2004; Li et al. 2011; Xu et al. 2012). Hence, it cannot be excluded that the observed growth decline of urea-grown *A. pseudogonyaulax* cells in this study may be partly attributed to insufficient nickel availability, as the employed K/2 media did not contain any additional nickel.

Nevertheless, the findings of this study suggest that urea is suboptimal for the growth of *A. pseudogonyaulax*, which is reinforced by the fact that urea-grown cultures could be easily recovered through the addition of nitrate or ammonium. Hence, it may be hypothesized that urea is not the primary driver of the observed expansion and proliferation of *A. pseudogonyaulax* in the eutrophic Danish Limfjord, despite the high levels of anthropogenic urea inputs induced by intensive agricultural farming (Glibert et al. 2005; Carlsson et al. 2009). However, the inability to utilize urea as a nitrogen source does not seem to be consistent with the well-known mixotrophic capabilities of *A. pseudogonyaulax* and the fact that maximum growth rates were only obtained in the presence of prey (Blossom et al. 2012, 2017). Nevertheless, the utilization of prey-based organic nitrogen has not been explicably shown for this dinoflagellate, which could be clarified by conducting isotope labeling studies such as for *A. catenella* (Kang and Gobler 2023).

Toxin normalization may have significant impacts on the interpretation of results

Studies generally normalize toxin quotas per cell, which can result in a loss of information since it excludes the effect of possible changes in the cell volume and intracellular carbon content, especially between the exponential and stationary GP (Supporting Information Table S3). Consequently, natural differences between both GPs are more likely resolved if toxin contents are normalized to another cell-specific feature such as the cell volume or carbon content. For instance, GDA (mol GDA mol^{-1} C^{-1}) in the exponential GP of the inorganic nitrogen treatments of strains A and B was still higher than in the stationary GP of the N-deplete and urea treatment, while lower if normalized per cell or volume (Supporting Information Fig. S2). Hence, additionally including normalization per carbon and volume may further facilitate the comparability of toxin abundances between studies and/or species and thereby improve the capacity to predict the toxic impact of HABs on ecosystems.

GP rather than nitrogen source drives toxin content of A. pseudogonyaulax

The influence of nitrogen availability on intracellular toxin abundances of PST-producing *Alexandrium* species exhibited a similar diverse pattern as the growth response toward nitrogen. For instance, Xu et al. (2012) reported either strong or only minor effects of differing nitrogen sources on the toxin content of different strains of *A. catenella* (note that Xu et al. reported one of the strains as *A. tamarense*). Modest effects of nitrogen sources on the toxin content of *A. catenella* were also reported by Leong et al. (2004) (reported as *A. tamarense*) and Li et al. (2011). In all three studies, no explicit correlation between GP (i.e., exponential or stationary GP) and toxin content was observed (Leong et al. 2004; Li et al. 2011; Xu et al. 2012). For *A. pseudogonyaulax*, toxin abundances of each treatment were higher in the stationary than in the

exponential GP, implying an accumulation of toxins toward the later stages of algae blooms and hence, potentially increased toxin exposure of other marine organisms and/or reduced grazing pressure toward *A. pseudogonyaulax*. However, during each GP, the nitrogen source did not substantially influence toxin levels, which is likely due to GDs not containing nitrogen. Another explanation may be that the activity of enzymes involved in GD production is independent of nitrogen. Consistently, previous research on PST-producing *A. catenella* generally found a stronger impact of the nitrogen source on the toxin content in agreement with PSP-toxins containing a substantial amount of nitrogen (Béchemin et al. 1999; Leong et al. 2004; Li et al. 2011; Xu et al. 2012). To unravel the relationship between GPs and toxin content, future studies should include multiple toxin sampling days within the same GP. This approach would enable the calculation of toxin production rates, offering additional insights alongside cellular toxin contents (Park et al. 2023).

Furthermore, *A. pseudogonyaulax* cultivated on inorganic nitrogen sources exhibited higher toxin contents compared to those grown on urea in accordance with previous studies observing similar trends with other PST-producing *Alexandrium* species (Leong et al. 2004; Li et al. 2011). This finding further emphasizes the limited significance of urea in assessing the future risk potential of *A. pseudogonyaulax* in northern European waters.

Intraspecific variabilities between two strains isolated at the same location

Even though strain A and strain B were isolated from the same location, intraspecific differences in growth rates, toxin and nutrient contents were found. These findings highlight the necessity to conduct laboratory experiments with multiple strains, especially if the results are subsequently processed in modeling studies featuring long-term predictions.

A. pseudogonyaulax *and the role of light*

Light intensity strongly affected growth and pigment composition

The growth rates of all three *A. pseudogonyaulax* strains increased concomitantly with increasing PFDs (Fig. 5), reflecting the interdependence of phototrophic growth rates and light intensity. More importantly, the relationship between growth rate and light (Fig. 6) suggests that *A. pseudogonyaulax* can grow in a wide range of light conditions. Similarly, studies have shown that *A. catenella* (Parkhill 1999; Etheridge and Roesler 2005; Laabir et al. 2011) (reported as *A. tamarense* and *A. fundyense* by Parkhill et al. and Etheridge et al., respectively), *A. minutum* (Hwang and Lu 2000) and *Alexandrium pohangense* (Lim et al. 2019) can also grow over broad light ranges and are tolerant toward high light (≥ 200 μmol photons $m^{-2}s^{-1}$) scenarios. In contrast, the growth of *A. ostenfeldii* exhibited a sharp maximum at 100 μmol photons $m^{-2}s^{-1}$ followed by a rapid decline (Maclean et al. 2003). Hence, differences in light tolerance may have contributed to the replacement of *A. ostenfeldii* by *A. pseudogonyaulax* in northern European waters. This is especially important in shallow and regularly stratified areas of the Danish Limfjord (Carstensen et al. 2007), in which algae are subjected to high light conditions (≥ 200 μmol photons $m^{-2}s^{-1}$) in surface waters during the summer months (Stæhr et al. 2020).

Furthermore, stagnating growth of cells exposed to LL conditions could be rapidly recovered by increasing the light intensity indicating that *A. pseudogonyaulax* cells can overcome longer periods of reduced light without decaying or forming resting stages. The LL conditions are representative of light conditions at 5 m depth (which reflects well the average water depth for the Limfjord) during summer month and surface waters during winter month in the Limfjord (Stæhr et al. 2020). Nonetheless, carbon acquisition via photosynthesis at LL was insufficient (except for strain A) to meet the cellular carbon demands for growth or, at LL, *A. pseudogonyaulax* may allocate carbon to other cellular processes apart from cell division. Notably, *A. pseudogonyaulax* cells in the LL treatment were acclimated at 60 μmol photons $m^{-2}s^{-1}$, instead of 20 μmol photons $m^{-2}s^{-1}$, and improved acclimatization protocols may enhance the capability of *A. pseudogonyaulax* to thrive in LL conditions. It was further observed that the ML and HL treatment reached two to three times higher cell densities in comparison to the nitrogen experiment. Factors governing the cell densities of dinoflagellates in the stationary phase are, however, still poorly understood. Since macronutrient concentrations were high, differences in cell densities may be explained by an increase in pH. Next to potentially affecting cellular processes directly, elevated pH reduces bicarbonate availability in the carbonate system leading to decreased carbon availability and growth (Hansen 2002; Hansen et al. 2007). Similarly, NO_3^- and NH_4^+ grown cultures in the nitrogen experiment may have also been carbon limited as intracellular carbon contents in the exponential and stationary GP were the same (Supporting Information Table S3). However, pH in the experiments was not measured and thus a relation between light and pH remains elusive and direct effects of light on maximum cell densities through unknown cellular mechanisms may have to be considered.

In addition to growth, light intensity strongly influenced the pigment composition of all three *A. pseudogonyaulax* strains. Pigment ratios in this study are in agreement with previously published results obtained for the same species by Zapata et al. (2012). Under LL conditions, cells upregulated the production of light-harvesting pigments (peridinin, Chl *a*, Chl c_2) and featured up to three times higher LH : LP ratios than ML or HL acclimatized cells (Supporting Information Table S5), a commonly observed acclimatization strategy of microalgae in response to higher light levels (Borowitzka et al. 2016).

Photophysiological response is largely independent of light intensities

The photophysiological response of *A. pseudogonyaulax* showed little variation in response to varying PFDs. Surprisingly, the maximum quantum yield of PSII ($F_v F_m^{-1}$) and high PSII normalized ETR were equal for all three treatments of strains B and C, and hence, it is unlikely that the photosynthetic apparatus was damaged at LL or HL conditions. High PSII normalized ETR that is not translated into cell growth for the LL treatment of strains B and C, may be explained by varying contributions of alternative electron pathways to overall ETR. Alternative electron pathways, such as the Mehler reaction, regulate the ATP/NADPH ratio in photosynthetic light reactions, but do not necessarily contribute to carbon fixation (Roberty et al. 2014). Unintuitively, LL acclimatized cells of strains B and C featured comparable ETR cell^{-1} as ML and HL acclimatized cells, but still did not sustain growth over the timeframe of the experiment. Conversely, the LL acclimatized strain A featured a lower ETR cell^{-1}, however, this strain did sustain growth over the timeframe of the experiment. High intraspecific variability in natural phytoplankton populations has already been observed, implicating the difficulty of abstracting results from monoclonal laboratory experiments onto natural populations and communities (Kremp et al. 2012; Wolf et al. 2018). Similarly, it may be hypothesized that the observed intraspecific variability regarding light increases the resilience of natural *A. pseudogonyaulax* communities toward environmental changes and hence strain A may be specifically adapted to LL scenarios or even to the winter season.

Thylakoid structure may influence diffusion of electron carriers

In plastids of green algae, the two photosystems (PSs) are segregated into different thylakoid subdomains. PSII is mostly located in the grana stacks, while PSI is mainly found in the stroma lamellae (Flori et al. 2017). No such thylakoid subdomains are visible in plastids of dinoflagellates (comparable to diatoms), where loose stacks of mostly three thylakoids are found. These different thylakoid architectures may differently affect the diffusion of the soluble electron carriers. While PSs confinement in subdomains constrains the electron flow in green algae, it may be hypothesized that the less structured thylakoids of dinoflagellates allow a faster diffusion of the soluble electron carriers and therewith a faster redox equilibration between the two PSs. In this study, increasing the rates for the mobile electron carriers in comparison with the original green algae model (Kroon and Thoms 2006) led to a better agreement of measured and modeled ETRs (Fig. 8), strengthening the aforementioned hypothesis.

Depressed growth at low light may indicate a switch to mixotrophic feeding

Interestingly, Lim et al. (2019) reported a significantly lower light compensation point of *A. pohangense* cultures grown mixotrophic compared with phototrophic growth, indicating that ingested prey can serve as a substitute for cellular carbon demands under LL conditions. Factors governing the balance between phototrophic and phagotrophic nutrition modes in mixoplankton species in response to light are, however, not fully understood (Hansen 2011; Flynn et al. 2019; Jeong et al. 2021). While it is known that many mixotrophic dinoflagellates are dependent on light to feed (Hansen 2011), even highly mixotrophic species such as *Karlodinium* spp. (Berge and Hansen 2016), the underlying causality is unclear. For phagotrophy of *A. pseudogonyaulax*, Blossom et al. (2012) reported an exceptional feeding mechanism that involves the production of extracellular mucus traps. These substances, even though not structurally elucidated yet, are large carbon-based macromolecules and hence it may be speculated that their biosynthesis is competing with cell division (Long et al. 2021) and that, below a certain light intensity, the biosynthesis of substances aiding in feeding may impede phototrophic driven cell division of *A. pseudogonyaulax*.

Growth stage rather than light drives toxin content of A. pseudogonyaulax

The relationship between light availability and toxin quotas in *Alexandrium* populations is as versatile as the relationship between macronutrient concentrations and toxin quotas. Different studies on the influence of bottom-up factors on the toxin content of microalgae have reported direct, inverse, and no systematic relationships between PFDs and toxin quotas, highlighting the complexity of cellular toxicity (Parkhill 1999; Maclean et al. 2003; Wang and Hsieh 2005; Laabir et al. 2013). For *A. minutum* and *A. catenella*, the highest PST quotas have also been found at ML intensities resulting in a Gaussian-like relationship between PFDs and toxin quotas (Parkhill 1999; Hwang and Lu 2000). The present study cannot resolve such uncertainties due to a lack of a systematic relationship between PFDs and toxin contents (Fig. 7). Instead, a trend similar to the nitrogen experiment (Fig. 3) was observed with significantly higher toxin quotas in the stationary compared to the exponential GP. These differences, however, were less apparent if toxin contents were normalized per volume instead of per cell (Supporting Information Fig. S3), underlining how toxin normalization may influence the interpretation of results. In addition, toxin contents decreased from strain C to strain A and then to strain B, revealing substantial intraspecific variability. Consequently, the potential adverse effects of *A. pseudogonyaulax* blooms may vary significantly based on the dominant strain within the blooming community. Altogether, these findings suggest that toxin abundances in *A. pseudogonyaulax* are influenced by multiple factors, including light availability and GP, and that the relationship between light intensity and toxin production is complex.

Conclusions

The findings of this study show that the growth rate of the harmful algae bloom dinoflagellate *A. pseudogonyaulax* was significantly influenced by nitrogen source and light intensity, both important drivers of bloom formation. Meanwhile, the intracellular toxin content was predominantly driven by the growth stage. In addition, considerable physiological intraspecific variability of different *A. pseudogonyaulax* strains have been observed, thus emphasizing the importance of conducting laboratory experiments using multiple monoclonal strains. The study further suggests that the observed expansion and proliferation of *A. pseudogonyaulax* in the Danish Limfjord cannot be attributed to high anthropogenic urea inputs, while a broad light tolerance may have favored it. Altogether, the findings point toward a long-term establishment of *A. pseudogonyaulax* in northern European waters. Considering the ongoing expansion of this toxic dinoflagellate, further research into other bottom-up factors (e.g., salinity, temperature, mixotrophy) and their influence on the toxicity of *A. pseudogonyaulax* are needed.

Data availability statement

All data needed to evaluate the conclusions in the paper are present in the paper and/or supporting information and are freely available from the PANGAEA data repository: https://doi.pangaea.de/10.1594/PANGAEA.965195. All code can be found online on GitHub: https://github.com/KristofM854 (accessed on 18 April 2024).

References

Anderson, D. M. 2009. Approaches to monitoring, control and management of harmful algal blooms (HABs). Ocean Coast. Manag. **52**: 342–347. doi:10.1016/j.ocecoaman.2009.04.006

Anderson, D. M., P. M. Glibert, and J. M. Burkholder. 2002. Harmful algal blooms and eutrophication: Nutrient sources, composition, and consequences. Estuaries **25**: 704–726. doi:10.1007/BF02804901

Armstrong, C., D. Erdner, J. McClelland, M. Sanderson, D. Anderson, C. Gobler, and J. Smith. 2018. Impact of nitrogen chemical form on the isotope signature and toxicity of a marine dinoflagellate. Mar. Ecol. Prog. Ser. **602**: 63–76. doi:10.3354/meps12619

Arnold, J. B. 2021. ggthemes: Extra Themes, Scales and Geoms for 'ggplot2'.

Béchemin, C., D. Grzebyk, F. Hachame, C. Hummert, and S. Maestrini. 1999. Effect of different nitrogen/phosphorus nutrient ratios on the toxin content in *Alexandrium minutum*. Aquat. Microb. Ecol. **20**: 157–165. doi:10.3354/ame020157

Benjamini, Y., and Y. Hochberg. 1995. Controlling the false discovery rate: A practical and powerful approach to multiple testing. J. R. Stat. Soc.: B Methodol. **57**: 289–300. doi:10.1111/j.2517-6161.1995.tb02031.x

Berge, T., and P. Hansen. 2016. Role of the chloroplasts in the predatory dinoflagellate *Karlodinium armiger*. Mar. Ecol. Prog. Ser. **549**: 41–54. doi:10.3354/meps11682

Biecheler, B. 1952. Recherches sur les Peridiniens. Bull. Biol. Fr. Belg. **36**: 1–149.

Blossom, H. E., N. Daugbjerg, and P. J. Hansen. 2012. Toxic mucus traps: A novel mechanism that mediates prey uptake in the mixotrophic dinoflagellate *Alexandrium pseudogonyaulax*. Harmful Algae **17**: 40–53. doi:10.1016/j.hal.2012.02.010

Blossom, H. E., T. D. Bædkel, U. Tillmann, and P. J. Hansen. 2017. A search for mixotrophy and mucus trap production in *Alexandrium* spp. and the dynamics of mucus trap formation in *Alexandrium pseudogonyaulax*. Harmful Algae **64**: 51–62. doi:10.1016/j.hal.2017.03.004

Borowitzka, M. A., J. Beardall, and J. A. Raven [eds.]. 2016. The physiology of microalgae. Springer International Publishing. doi:10.1007/978-3-319-24945-2

Bronk, D. A., J. H. See, P. Bradley, and L. Killberg. 2007. DON as a source of bioavailable nitrogen for phytoplankton. Biogeosciences **4**: 283–296. doi:10.5194/bg-4-283-2007

Burson, A., M. Stomp, L. Akil, C. P. D. Brussaard, and J. Huisman. 2016. Unbalanced reduction of nutrient loads has created an offshore gradient from phosphorus to nitrogen limitation in the North Sea. Limnol. Oceanogr. **61**: 869–888. doi:10.1002/lno.10257

Carlsson, M. S., M. Holmer, and J. K. Petersen. 2009. Seasonal and spatial variations of benthic impacts of mussel longline farming in a eutrophic Danish Fjord, Limfjorden. J. Shellfish Res. **28**: 791–801. doi:10.2983/035.028.0408

Carstensen, J., P. Henriksen, and A.-S. Heiskanen. 2007. Summer algal blooms in shallow estuaries: Definition, mechanisms, and link to eutrophication. Limnol. Oceanogr. **52**: 370–384. doi:10.4319/lo.2007.52.1.0370

Carstensen, J., D. Krause-Jensen, S. Markager, K. Timmermann, and J. Windolf. 2013. Water clarity and eelgrass responses to nitrogen reductions in the eutrophic Skive Fjord, Denmark. Hydrobiologia **704**: 293–309. doi:10.1007/s10750-012-1266-y

Chang, W. 2023. extrafont: Tools for using fonts.

Chomérat, N., C. M. Iti Gatti, É. Nézan, and M. Chinain. 2017. Studies on the benthic genus *Sinophysis* (Dinophysales, Dinophyceae) II. *S. canaliculata* from Rapa Island (French Polynesia). Phycologia **56**: 193–203. doi:10.2216/16-96.1

Cochlan, W. P., and P. J. Harrison. 1991. Uptake of nitrate, ammonium, and urea by nitrogen-starved cultures of *Micromonas pusilla* (Prasinophyceae): Transient responses. J. Phycol. **27**: 673–679. doi:10.1111/j.0022-3646.1991.00673.x

Coyne, K. J., L. R. Salvitti, A. M. Mangum, G. Ozbay, C. R. Main, Z. M. Kouhanestani, and M. E. Warner. 2021. Interactive effects of light, CO2 and temperature on growth and resource partitioning by the mixotrophic dinoflagellate,

Karlodinium veneficum. PLoS One **16**: e0259161. doi:10.1371/journal.pone.0259161

Dawson, C. 2022. ggprism: A 'ggplot2' extension inspired by 'GraphPad Prism'.

Dyhrman, S. T., and D. M. Anderson. 2003. Urease activity in cultures and field populations of the toxic dinoflagellate *Alexandrium*. Limnol. Oceanogr. **48**: 647–655. doi:10.4319/lo.2003.48.2.0647

Espiña, B., E. Cagide, M. C. Louzao, N. Vilariño, M. R. Vieytes, Y. Takeda, M. Sasaki, and L. M. Botana. 2016. Cytotoxicity of goniodomin A and B in non contractile cells. Toxicol. Lett. **250–251**: 10–20. doi:10.1016/j.toxlet.2016.04.001

Etheridge, S. M., and C. S. Roesler. 2005. Effects of temperature, irradiance, and salinity on photosynthesis, growth rates, total toxicity, and toxin composition for *Alexandrium fundyense* isolates from the Gulf of Maine and Bay of Fundy. Deep-Sea Res. II: Top. Stud. Oceanogr. **52**: 2491–2500. doi:10.1016/j.dsr2.2005.06.026

Flori, S., and others. 2017. Plastid thylakoid architecture optimizes photosynthesis in diatoms. Nat. Commun. **8**: 15885. doi:10.1038/ncomms15885

Flynn, K. J., and others. 2019. Mixotrophic protists and a new paradigm for marine ecology: Where does plankton research go now? J. Plankton Res. **41**: 375–391. doi:10.1093/plankt/fbz026

Frederiksen, M., M. Edwards, A. J. Richardson, N. C. Halliday, and S. Wanless. 2006. From plankton to top predators: Bottom-up control of a marine food web across four trophic levels. J. Anim. Ecol. **75**: 1259–1268. doi:10.1111/j.1365-2656.2006.01148.x

Furukawa, K., K. Sakai, S. Watanabe, K. Maruyama, M. Murakami, K. Yamaguchi, and Y. Ohizumi. 1993. Goniodomin A induces modulation of actomyosin ATPase activity mediated through conformational change of actin. J. Biol. Chem. **268**: 26026–26031. doi:10.1016/S0021-9258(19)74488-3

Glibert, P. M. 2016. Margalef revisited: A new phytoplankton mandala incorporating twelve dimensions, including nutritional physiology. Harmful Algae **55**: 25–30. doi:10.1016/j.hal.2016.01.008

Glibert, P. M., T. M. Trice, B. Michael, and L. Lane. 2005. Urea in the tributaries of the Chesapeake and Coastal Bays of Maryland. Water Air Soil Pollut. **160**: 229–243. doi:10.1007/s11270-005-2546-1

Gobler, C. J. 2020. Climate change and harmful algal blooms: Insights and perspective. Harmful Algae **91**: 101731. doi:10.1016/j.hal.2019.101731

Gobler, C. J., and others. 2011. Niche of harmful alga *Aureococcus anophagefferens* revealed through ecogenomics. Proc. Natl. Acad. Sci. USA **108**: 4352–4357. doi:10.1073/pnas.1016106108

Griffin, J. E., G. Park, and H. G. Dam. 2019. Relative importance of nitrogen sources, algal alarm cues and grazer exposure to toxin production of the marine dinoflagellate *Alexandrium catenella*. Harmful Algae **84**: 181–187. doi:10.1016/j.hal.2019.04.006

Hall, B. G., H. Acar, A. Nandipati, and M. Barlow. 2014. Growth rates made easy. Mol. Biol. Evol. **31**: 232–238. doi:10.1093/molbev/mst187

Hansen, P. 2002. Effect of high pH on the growth and survival of marine phytoplankton: Implications for species succession. Aquat. Microb. Ecol. **28**: 279–288. doi:10.3354/ame028279

Hansen, P. J. 2011. The role of photosynthesis and food uptake for the growth of marine mixotrophic Dinoflagellates: Mixotrophy in marine dinoflagellates. J. Eukaryot. Microbiol. **58**: 203–214. doi:10.1111/j.1550-7408.2011.00537.x

Hansen, P., N. Lundholm, and B. Rost. 2007. Growth limitation in marine red-tide dinoflagellates: Effects of pH versus inorganic carbon availability. Mar. Ecol. Prog. Ser. **334**: 63–71. doi:10.3354/meps334063

Harris, C. M., K. S. Reece, D. F. Stec, G. P. Scott, W. M. Jones, P. L. M. Hobbs, and T. M. Harris. 2020. The toxin goniodomin, produced by *Alexandrium* spp., is identical to goniodomin A. Harmful Algae **92**: 101707. doi:10.1016/j.hal.2019.101707

Harris, C. M., and others. 2023. Mass spectrometric characterization of the seco acid formed by cleavage of the macrolide ring of the algal metabolite goniodomin A. Toxicon **231**: 107159. doi:10.1016/j.toxicon.2023.107159

Heisler, J., and others. 2008. Eutrophication and harmful algal blooms: A scientific consensus. Harmful Algae **8**: 3–13. doi:10.1016/j.hal.2008.08.006

Hsia, M. H., S. L. Morton, L. L. Smith, K. R. Beauchesne, K. M. Huncik, and P. D. R. Moeller. 2006. Production of goniodomin A by the planktonic, chain-forming dinoflagellate *Alexandrium monilatum* (Howell) Balech isolated from the Gulf Coast of the United States. Harmful Algae **5**: 290–299. doi:10.1016/j.hal.2005.08.004

Hwang, D. F., and Y. H. Lu. 2000. Influence of environmental and nutritional factors on growth, toxicity, and toxin profile of dinoflagellate *Alexandrium minutum*. Toxicon **38**: 1491–1503. doi:10.1016/S0041-0101(00)00080-5

Jacox, M. G., E. L. Hazen, and S. J. Bograd. 2016. Optimal environmental conditions and anomalous ecosystem responses: Constraining bottom-up controls of phytoplankton biomass in the California Current System. Sci. Rep. **6**: 27612. doi:10.1038/srep27612

Jakobsen, H. H., and S. Markager. 2016. Carbon-to-chlorophyll ratio for phytoplankton in temperate coastal waters: Seasonal patterns and relationship to nutrients. Limnol. Oceanogr. **61**: 1853–1868. doi:10.1002/lno.10338

James, K. J., B. Carey, J. O'Halloran, F. N. A. M. van Pelt, and Z. Škrabáková. 2010. Shellfish toxicity: Human health implications of marine algal toxins. Epidemiol. Infect. **138**: 927–940. doi:10.1017/S0950268810000853

Jeong, H. J., and others. 2021. Feeding diverse prey as an excellent strategy of mixotrophic dinoflagellates for global

dominance. Sci. Adv. **7**: eabe4214. doi:10.1126/sciadv.abe4214

Kang, Y., and C. J. Gobler. 2023. Nitrogen liberated via allelopathy can promote harmful algal blooms. Harmful Algae **129**: 102490. doi:10.1016/j.hal.2023.102490

Karlson, B., and others. 2021. Harmful algal blooms and their effects in coastal seas of Northern Europe. Harmful Algae **102**: 101989. doi:10.1016/j.hal.2021.101989

Kassambara, A. 2023*a*. rstatix: Pipe-friendly framework for basic statistical tests.

Kassambara, A. 2023*b*. ggpubr: 'ggplot2' Based Publication Ready Plots.

Keller, M. D., R. C. Selvin, W. Claus, and R. R. L. Guillard. 2007. Media for the culture of oceanic ultraphytoplankton. J. Phycol. **23**: 633–638. doi:10.1111/j.1529-8817.1987.tb04217.x

Kremp, A., A. Godhe, J. Egardt, S. Dupont, S. Suikkanen, S. Casabianca, and A. Penna. 2012. Intraspecific variability in the response of bloom-forming marine microalgae to changed climate conditions: Phenotypic variability and climate conditions. Ecol. Evol. **2**: 1195–1207. doi:10.1002/ece3.245

Kremp, A., and others. 2019. Distributions of three *Alexandrium* species and their toxins across a salinity gradient suggest an increasing impact of GDA producing *A. pseudogonyaulax* in shallow brackish waters of Northern Europe. Harmful Algae **87**: 101622. doi:10.1016/j.hal.2019.101622

Kroon, B. M. A., and S. Thoms. 2006. From electron to biomass: A mechanistic model to describe phytoplankton photosynthesis and steady-state growth rates. J. Phycol. **42**: 593–609. doi:10.1111/j.1529-8817.2006.00221.x

Laabir, M., and others. 2011. Influence of temperature, salinity and irradiance on the growth and cell yield of the harmful red tide dinoflagellate *Alexandrium catenella* colonizing Mediterranean waters. J. Plankton Res. **33**: 1550–1563. doi:10.1093/plankt/fbr050

Laabir, M., Y. Collos, E. Masseret, D. Grzebyk, E. Abadie, V. Savar, M. Sibat, and Z. Amzil. 2013. Influence of environmental factors on the paralytic shellfish toxin content and profile of *Alexandrium catenella* (Dinophyceae) isolated from the Mediterranean Sea. Mar. Drugs **11**: 1583–1601. doi:10.3390/md11051583

Leong, S. C. Y., A. Murata, Y. Nagashima, and S. Taguchi. 2004. Variability in toxicity of the dinoflagellate *Alexandrium tamarense* in response to different nitrogen sources and concentrations. Toxicon **43**: 407–415. doi:10.1016/j.toxicon.2004.01.015

Levasseur, M., P. A. Thompson, and P. J. Harrison. 1993. Physiological acclimation of marine phytoplankton to different nitrogen sources. J. Phycol. **29**: 587–595. doi:10.1111/j.0022-3646.1993.00587.x

Li, T.-S., R.-C. Yu, and M.-J. Zhou. 2011. Short-term effects of different nitrogen substrates on growth and toxin production of dinoflagellate *Alexandrium catenella* Balech (strain ACDH). Harmful Algae **12**: 46–54. doi:10.1016/j.hal.2011.08.011

Lim, A. S., H. J. Jeong, J. H. Ok, J. H. You, H. C. Kang, and S. J. Kim. 2019. Effects of light intensity and temperature on growth and ingestion rates of the mixotrophic dinoflagellate *Alexandrium pohangense*. Mar. Biol. **166**: 98. doi:10.1007/s00227-019-3546-9

Long, M., B. Krock, J. Castrec, and U. Tillmann. 2021. Unknown extracellular and bioactive metabolites of the genus *Alexandrium*: A review of overlooked toxins. Toxins **13**: 905. doi:10.3390/toxins13120905

Ma, H., B. Krock, U. Tillmann, U. Bickmeyer, M. Graeve, and A. Cembella. 2011. Mode of action of membrane-disruptive lytic compounds from the marine dinoflagellate *Alexandrium tamarense*. Toxicon **58**: 247–258. doi:10.1016/j.toxicon.2011.06.004

Maclean, C., A. D. Cembella, and M. A. Quilliam. 2003. Effects of light, salinity and inorganic nitrogen on cell growth and Spirolide production in the marine dinoflagellate *Alexandrium ostenfeldii* (Paulsen) Balech et Tangen. Bot. Mar. **46**: 466–476. doi:10.1515/BOT.2003.048

May, S. P., J. M. Burkholder, S. E. Shumway, H. Hégaret, G. H. Wikfors, and D. Frank. 2010. Effects of the toxic dinoflagellate *Alexandrium monilatum* on survival, grazing and behavioral response of three ecologically important bivalve molluscs. Harmful Algae **9**: 281–293. doi:10.1016/j.hal.2009.11.005

Ogata, T., T. Ishimaru, and M. Kodama. 1987. Effect of water temperature and light intensity on growth rate and toxicity change in *Protogonyaulax tamarensis*. Mar. Biol. **95**: 217–220. doi:10.1007/BF00409008

Park, G., L. Norton, D. Avery, and H. G. Dam. 2023. Grazers modify the dinoflagellate relationship between toxin production and cell growth. Harmful Algae **126**: 102439. doi:10.1016/j.hal.2023.102439

Parkhill, J. 1999. Effects of salinity, light and inorganic nitrogen on growth and toxigenicity of the marine dinoflagellate *Alexandrium tamarense* from northeastern Canada. J. Plankton Res. **21**: 939–955. doi:10.1093/plankt/21.5.939

Pedersen, T. L. 2024. patchwork: The composer of plots.

Petzoldt, T. 2022. growthrates: Estimate growth rates from experimental data.

R Core Team. 2021. R: A language and environment for statistical computing. R Foundation for Statistical Computing.

Rinker, T. W., and D. Kurkiewicz. 2018. pacman: Package management for R.

Roberty, S., B. Bailleul, N. Berne, F. Franck, and P. Cardol. 2014. PSI Mehler reaction is the main alternative photosynthetic electron pathway in *Symbiodinium* sp., symbiotic dinoflagellates of cnidarians. New Phytol. **204**: 81–91. doi:10.1111/nph.12903

Rodrigues-Sanchez, F., and C. P. Jackson. 2023. grateful: Facilitate citation of R packages.

Sharma, G. M., L. Michaels, and P. R. Burkholder. 1968. Goniodomin, a new antibiotic from a dinoflagellate. J. Antibiot. **21**: 659–664. doi:10.7164/antibiotics.21.659

Soetaert, K., and T. Petzoldt. 2010. Inverse modelling, sensitivity and Monte Carlo analysis in R using package FME. J. Stat. Softw. **33**: 1–28. doi:10.18637/jss.v033.i03

Stæhr, P. A., S. Markager, S. Høgslund, J. W. Hansen, D. Tonetta, S. Upadhyay, and M. Møller Nielsen. 2020. Stenrev som muligt kvælstofvirkemiddel: Vækstbetingelser for bentiske alger og deres betydning for ilt- og næringsstofdynamikken i Limfjorden. Rapport Aarhus Universitet.

Terao, K., E. Ito, M. Murakami, and K. Yamaguchi. 1989. Histopathological studies on experimental marine toxin poisoning—III. Morphological changes in the liver and thymus of male ICR mice induced by goniodomin A, isolated from the dinoflagellate *Goniodoma pseudogoniaulax*. Toxicon **27**: 269–271. doi:10.1016/0041-0101(89)90141-4

Thompson, P. A., M. E. Levasseur, and P. J. Harrison. 1989. Light-limited growth on ammonium vs. nitrate: What is the advantage for marine phytoplankton? Limnol. Oceanogr. **34**: 1014–1024. doi:10.4319/lo.1989.34.6.1014

Wang, D.-Z., and D. P. H. Hsieh. 2005. Growth and toxin production in batch cultures of a marine dinoflagellate *Alexandrium tamarense* HK9301 isolated from the South China Sea. Harmful Algae **4**: 401–410. doi:10.1016/j.hal.2004.07.002

Wickham, H., and others. 2019. Welcome to the tidyverse. J. Open Source Softw. **4**: 1686. doi:10.21105/joss.01686

Wilke, C. O., and B. M. Wiernik. 2022. ggtext: Improved Text Rendering Support for 'ggplot2'.

Wolf, K. K. E., C. J. M. Hoppe, and B. Rost. 2018. Resilience by diversity: Large intraspecific differences in climate change responses of an Arctic diatom: Intraspecific differences in an Arctic diatom. Limnol. Oceanogr. **63**: 397–411. doi:10.1002/lno.10639

Xu, J., and others. 2012. Effects of inorganic and organic nitrogen and phosphorus on the growth and toxicity of two *Alexandrium* species from Hong Kong. Harmful Algae **16**: 89–97. doi:10.1016/j.hal.2012.02.006

Zapata, M., S. Fraga, F. Rodríguez, and J. Garrido. 2012. Pigment-based chloroplast types in dinoflagellates. Mar. Ecol. Prog. Ser. **465**: 33–52. doi:10.3354/meps09879

Zmerli Triki, H., M. Laabir, and O. Kéfi Daly-Yahia. 2015. Life history, excystment features, and growth characteristics of the Mediterranean harmful dinoflagellate *Alexandrium pseudogonyaulax*. J. Phycol. **51**: 980–989. doi:10.1111/jpy.12337

Zmerli Triki, H., M. Laabir, P. Moeller, N. Chomérat, and O. Kéfi Daly-Yahia. 2016. First report of goniodomin A production by the dinoflagellate *Alexandrium pseudogonyaulax* developing in southern Mediterranean (Bizerte Lagoon, Tunisia). Toxicon **111**: 91–99. doi:10.1016/j.toxicon.2015.12.018

Acknowledgments

Financial support for K. Möller was provided by the Deutsche Bundesstiftung Umwelt (DBU). We wish to thank our colleagues Annegret Müller and Thomas Max for various practical assistance and Ingrid Stimac and Sandra Murawski for assisting with the nutrient analysis. We further acknowledge the helpful input by our reviewers. Open Access funding enabled and organized by Projekt DEAL.

Conflict of interest

None declared.

Submitted 24 August 2023
Revised 02 April 2024
Accepted 05 April 2024

Associate editor: Michele Burford